

Perineuronal nets increase inhibitory GABAergic currents during the critical period in rats

Hui Liu^{1,2}, Peng-Fen Gao^{1,2}, Hai-Wei Xu^{1,2}, Ming-Ming Liu^{1,2}, Tao Yu^{1,2}, Jun-Ping Yao^{1,2}, Zheng-Qin Yin^{1,2}

Foundation item: National Natural Sciences Foundation of China (No. 81070749)

¹Southwest Eye Hospital, Southwest Hospital, Third Military Medical University, Chongqing 400038, China

²Key Lab of Visual Damage and Regeneration & Restoration of Chongqing, Chongqing 400038, China

Correspondence to: Zheng-Qin Yin. Southwest Eye Hospital, Southwest Hospital, Third Military Medical University, Chongqing 400038, China. qinzyin@yahoo.com.cn

Received: 2012-10-23

Accepted: 2013-03-10

Abstract

• **AIM:** To investigate inhibitory γ -aminobutyric acid (GABA) ergic postsynaptic currents (IPSCs) and postsynaptic currents (PSCs) in layer IV of the rat visual cortex during the critical period and when plasticity was extended through dissolution of the perineuronal nets (PNNs).

• **METHODS:** We employed 24 normal Long–Evans rats to study GABA_A–PSC characteristics of neurons within layer IV of the visual cortex during development. The animals were divided into six groups of four rats according to ages at recording: PW3 (P21–23d), PW4 (P28–30d), PW5 (P35–37d), PW6 (P42–44d), PW7 (P49–51d), and PW8 (56–58d). An additional 24 chondroitin sulfate proteoglycan (CSPG) degradation rats (also Long–Evans) were generated by making a pattern of injections of chondroitinase ABC (chABC) into the visual cortex 1 week prior to recording at PW3, PW4, PW5, PW6, PW7, and PW8. Immunohistochemistry was used to identify the effect of chABC injection on CSPGs. PSCs were detected with whole–cell patch recordings, and GABA_A receptor–mediated IPSCs were pharmacologically isolated.

• **RESULTS:** IPSC peak current showed a strong rise in the age–matched control group, peaked at PW5 and were maintained at a roughly constant value thereafter. Although there was a small increase in peak current for the chABC group with age, the peak currents continued to decrease with the delayed highest value at PW6, resulting in significantly different week–by–week comparison with normal development. IPSC decay time continued to increase until PW7 in the control group, while those in the chABC group were maintained at a

stable level after an initial increase at PW4. Compared with normal rats, the decay times recorded in the chABC rats were always shorter, which differed significantly at each age. We did not observe any differences in IPSC properties between the age–matched control and penicillinase (P–ase) group. However, the change in IPSCs after chABC treatment was not reflected in the total PSCs or in basic membrane properties in layer IV of the rat visual cortex.

• **CONCLUSION:** Our results demonstrate that rather than rapidly increasing during the critical period for neuronal plasticity, IPSCs in layer IV of rat visual cortex are maintained at an immature level when PNNs are removed by chABC. This suggests that GABA receptor maturation involves the conformation of the CSPGs in PNNs.

• **KEYWORDS:** gamma-aminobutyric acid receptor; plasticity; visual cortex; development; postsynaptic currents; chondroitinase ABC; chondroitin sulfate proteoglycans; whole-cell patch recording

DOI:10.3980/j.issn.2222–3959.2013.02.02

Liu H, Gao PF, Xu HW, Liu MM, Yu T, Yao JP, Yin ZQ. Perineuronal nets increase inhibitory GABAergic currents during the critical period in rats. *Int J Ophthalmol* 2013;6(2):120–125

INTRODUCTION

The mammalian visual cortex is highly susceptible to experience-dependent modifications to structural and functional architecture during the critical period in early postnatal development^[1,2]. However, visual plasticity is drastically reduced after the critical period. γ -aminobutyric acid (GABA) inhibitory circuits are implicated in critical-period initiation and termination during visual cortex development^[3–5]. Recently, the concept of drastically attenuated plasticity after the critical period has been revised by evidence of reactivation of plasticity in adult rodent visual cortex when monocular deprivation (MD) is preceded by visual deprivation^[6]. Critical-period onset can also be delayed when GABA release is kept at a low level by gene-targeted disruption of the synaptic isoform of its synthetic enzyme, glutamic acid decarboxylase 65 (GAD65)^[3]. Conversely, the natural plasticity process is accelerated by prematurely enhancing inhibition^[3,5], with GABA itself being described as

a self-limiting trophic substance during development^[7]. However, how does GABA inhibitory synaptic transmission change during development in normal and abnormal visual environments? To date, this question remains unanswered.

Pizzorusso *et al*^[8] successfully restored adult rat visual cortical plasticity by dissolving chondroitin sulfate proteoglycan (CSPG) glycosaminoglycan (GAG) chains in perineuronal nets (PNNs) with chondroitinase ABC (chABC). In the rat visual cortex, CSPG condensation in PNNs increases with development and is completed around the end of the critical period, after which it is kept at a constant mature level^[8-10]. Moreover, developmental maturation of CSPGs may contribute to the progressive reduction of plasticity, as well as critical-period termination^[8,11-13]. Yet, the mechanisms by which CSPGs inhibit plasticity in the adult visual cortex remain unknown. Berardi *et al*^[14] speculated that CSPG elimination allows for greater spine motility, and hence, greater plasticity. Interestingly, cortical PNNs have been associated with GABAergic neurons^[8], with the $\alpha 1$ subunit being the most abundant form of the GABA_A receptor^[15]. Thus, the functional relationship between CSPGs and GABA_A inhibitory circuits needs to be clarified.

To investigate these questions, we studied rats with ages spanning the beginning and termination of the critical period and established a CSPG degradation model with multiple injections of chABC in the right visual cortex. We recorded post-synaptic currents (PSCs) from layer IV neurons in visual cortical slices with whole-cell patch-clamp recording and pharmacologically isolated GABA_A receptor-mediated inhibitory postsynaptic currents (IPSCs) to explore the synaptic and cellular mechanisms of critical-period termination in the visual cortex.

MATERIALS AND METHODS

Animal Preparation Visual cortical slices were prepared from Long-Evans rats of both genders. All rats were bred by the Animal Care Center, Daping Hospital/Research Institute of Surgery, Chongqing, China. They were reared in a light-controlled room (90lx from 08:00 to 20:00 hours^[16]). All procedures used here accorded with the Guidance Suggestions for the Care and Use of Laboratory Animals formulated by the Ministry of Science and Technology of the People's Republic of China.

We employed 24 normal Long-Evans rats between postnatal day 21 and 56 (P21-56d) to study GABA_A-IPSC characteristics within layer IV of the visual cortex during development. The animals were divided into six groups of four rats according to ages at recording: PW3 (P21-23d), PW4 (P28-30d), PW5 (P35-37d), PW6 (P42-44d), PW7 (P49-51d), and PW8 (56-58d).

We generated 24 CSPG degradation rats (Long-Evans) and 24 penicillinase (P-ase) control rats by making a pattern of protease-free chABC (C2905, Sigma, St. Louis, MO, USA) or P-ase injections into the right visual cortex beginning at

P14d, P21d, P28d, P35d, P42d, or P49d, 1 week prior to recording at PW3, PW4, PW5, PW6, PW7, or PW8. The animals were anesthetized with intraperitoneal ketamine/xylazine (50mg/10mg/kg, *i.p.*). We then performed 750-nl injections of a 48 units/mL solution of chABC or P-ase at five locations surrounding the rat primary visual cortex with a glass pipette (30- μ m tip diameter) mounted on a motorized (0.1- μ m step) three-axis micromanipulator connected to an injector^[8]. With respect to lambda, the five locations were: 3.8-mm lateral and 1-mm posterior, 3.8-mm lateral and 1-mm anterior, 6.2-mm lateral and 1-mm posterior, 6.2-mm lateral and 1-mm anterior, and 5-mm lateral and 2-mm anterior. For each location, 375-nl was injected at two different depths (350 and 750 μ m). Injections were repeated at the same sites every 3 days. The recording and histological assessment zones were performed at least 1mm from the injection sites. Seven days after the first injections, animals were sacrificed, and samples were prepared for patch-clamp whole-cell recording and histological assessments.

To investigate the effect of chABC injection on CSPGs, six rats (one from each group) were perfused with 4% paraformaldehyde in phosphate buffer, and visual cortices were post-fixed for 2 hours before being placed in 30% sucrose in phosphate-buffered saline (PBS). Then, 40- μ m transverse sections from the occipital cortex were initially incubated for 1 hour in a solution composed of 20mmol/L lysine and 0.5% Triton-X-100 in PBS, pH 7.4. The sections were subsequently incubated overnight at 4°C in anti-neurocan monoclonal antibody (1:100; Chemicon, Temecula, CA, USA), followed by incubation with biotinylated anti-mouse antibody (1:20) for 40 minutes, and incubation in peroxidase anti-peroxidase complexes for 1 hour. Our results showed that there were no neurocan-labeled cells in the chABC-treated area, indicating that the chABC injections were effective (Figure 1).

The sections were also incubated overnight at 4°C with bio-WFA (biocytin-conjugated wisteria floribunda agglutinin) (1:200; Vector Laboratories, Burlingame, CA, USA), which binds CSPG glycosaminoglycan chains. After rinsing in PBS, the sections were processed for 1 hour at 37°C with Cy3-conjugated extravidin. The tissue was extensively washed with PBS, briefly placed in distilled water, mounted on fluorescence-free slides, air-dried, and coverslipped with Entellan. The slides were inspected using a confocal laser scanning microscope (Leica TCS 4D, Zeiss LSM 510; Wetzlar, Germany) with excitation parameters for Cy3 (550nm) (Figure 1).

Electrophysiological Recording Brain slice preparation: Animals were anaesthetized with ketamine/xylazine (50mg/10mg/kg, *i.p.*), and then decapitated. The brains were rapidly removed and placed in cold (4°C) artificial cerebrospinal fluid [ACSF; composition in mmol/L: 124 NaCl, 3 KCl, 2.4 CaCl₂, 1.3 MgSO₄, 1.25 NaH₂PO₄, 26 NaHCO₃, 10

D-glucose, aerated with 95% O₂ and 5% CO₂ (pH 7.4)]. Visual cortical coronal slices were cut at 300µm with a vibroslicer (Ted Pella Instruments, Redding, CA, USA), and were incubated at room temperature >1 hour in carbogenated ACSF. For electrophysiological recording, slices were superfused in a recording chamber with ACSF (3-4mL/minutes) maintained at 18-22°C.

Electrode preparation Pipettes were pulled from borosilicate glass capillaries using a P-97 micropipette puller (Sutter Instrument Co., Novato, CA, USA) and had a tip impedance of 5-10MΩ when filled with a solution containing (in mmol/L): 110 K-gluconate, 10 KCl, 5 NaCl, 1.5 MgCl₂, 20 HEPES, 0.5 EGTA (pH 7.3). The pipette was advanced to layer IV^[17], and a stainless steel bipolar stimulating electrode was placed into the center of white matter under a DVC video system. Whole-cell recordings from active neurons in layer IV of the visual cortex were performed under infrared differential interference contrast optics (IR-DIC).

Whole-cell patch-clamp recording Whole-cell patch-clamp recording was achieved using an Axoclamp-200B amplifier (Axon Instruments, Union City, CA, USA). PSCs were evoked with current pulses (0.5mA for 100µs) with the voltage clamped at -70mV. PSCs were recorded and averaged in each cell (Figure 1A). Miniature and evoked PSCs were acquired at 10-kHz sample frequency and filtered at half the acquisition rate with an eight-pole low-pass Bessel filter. Input resistance was measured in response to hyperpolarizing pulses of 0.05-0.1nA^[18]. Series resistance (10-20MΩ) was compensated and verified throughout the experiments.

GABA_A-IPSCs isolation GABA_A-IPSCs were isolated by adding D, L-2-amino-5-phosphonovalerate (AP-5, 50µmol/L, Sigma) and 6-cyano-7-nitroquinoxaline-2,3-dione (CNQX, 20µmol/L, Sigma) in the bathing medium for at least 5 minutes, which was sufficient to block N-methyl-D-aspartate (NMDA) and α-amino-3-hydroxy-5-methyl-4-isoxazolepropionic acid (AMPA) receptors, respectively. GABA_A-IPSCs were also tested by adding bicuculline methiodide (BMI, 20µmol/L, Sigma), CNQX (20µmol/L), and AP-5 (50µmol/L) to the ACSF to block GABA, AMPA, and NMDA receptors. Finally, all blockers were washed out for 15 minutes to test PSC recovery (Figure 1).

Statistical Analysis Curve fitting and data analysis were carried out with Clampfit 8.1 (Axon Instruments), SigmaPlot 8.0, and SPSS software (Ver. 11.5, SPSS Inc., Chicago, IL, USA). We measured the peak amplitudes, the decay time constants with a single exponential fit, input resistance (IR), and resting membrane potential (RMP)^[19]. Values (mean ± SE) were tested using separate analyses of variance (ANOVA) with Dunnett's posthoc tests to assess differences between variables.

RESULTS

Electrophysiological characteristics of layer IV neurons in normal rats during development Postsynaptic currents were recorded from layer IV of the rat visual cortex (PW3-8) with the membrane potential clamped at -70mV and with a stimulation intensity of 0.5mA. A total of 48 cells were patched from slices from normal rats, and 42 cells were patched from chABC rats or P-ase rats. Isolation of GABA_A-PSCs from layer IV neuron in rat visual cortex is illustrated in Figure 1.

Inhibitory currents were revealed by blocking NMDA and AMPA receptors through the addition of AP-5 (50µmol/L) and CNQX (20µmol/L), respectively, to the perfusion solution for at least 5 minutes. The GABAergic nature of the remnant PSCs was demonstrated by additionally blocking GABA_A receptors with the antagonist BMI (20µmol/L). Almost complete recovery of PSCs could be demonstrated by washing out the blockers. The chABC injections were made in a pattern so as to cover a significant portion of the right primary visual cortex. The dramatic degradation effect of chABC on PNNs is shown in Figure 1. At higher magnification, the PNNs are clearly visible surrounding the neuronal somata (Figure 1) of PW6 rat. However, PNNs are not visible in cortical regions where chABC was injected (Figure 1).

IPSCs GABAergic IPSCs were recorded *via* the techniques illustrated in Figure 1 and described in the Methods. IPSC peak current showed a strong rise in the normal group rat pups from PW3 to PW5 ($P < 0.05$, PW3 vs PW4; $P < 0.01$, PW4 vs PW5), then maintained at a roughly constant value over the subsequent period (Figure 2). In contrast, IPSCs did not exhibit such a strong increase at PW4 in the chABC group ($P > 0.05$, PW3 vs PW4); only at PW6 did IPSCs in the chABC group significantly exceed that at the earlier age ($P < 0.05$, PW5 vs PW6) (Figure 2). After PW3, the peak currents were always lower in the chABC group, resulting in significantly different week-by-week comparison with normal development through PW8 ($P < 0.01$, PW4-PW8 normal vs chABC) (Figure 2). The age-matched control and P-ase groups were not significantly different ($P > 0.05$, PW3-PW8 normal vs P-ase).

IPSC decay time continued to increase until PW7 in normal ($P < 0.01$, PW5 vs PW6; $P > 0.05$, PW6 vs PW7); 2 weeks after the IPSC had reached the maximum at PW5. After an initial increase at PW4 ($P < 0.01$, PW3 vs PW4), the mean decay times for the chABC group were maintained at a stable level from PW4 to PW8 ($P > 0.05$, PW4 vs PW8). Compared with the normal rats, the decay times recorded in slices from chABC rats were consistently shorter and differed significantly at each age ($P < 0.01$, PW3-PW8 normal vs chABC) (Figure 2). No difference was observed between the age-matched control and P-ase groups in IPSC decay times ($P > 0.05$, PW3-PW8, normal vs P-ase).

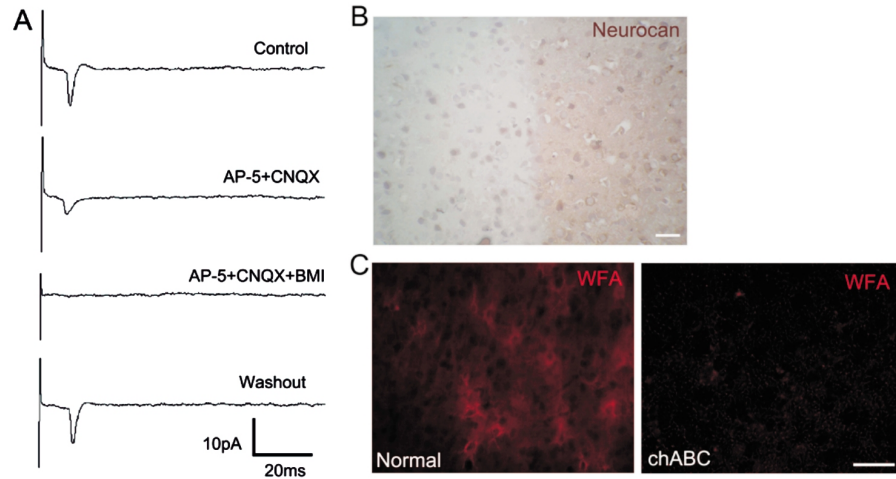


Figure 1 Establishment of IPSCs and effects of chABC injection into the visual cortex A: Isolation of IPSCs in a layer IV neuron; B: Neurocan staining after chABC treatment shows CSPG degradation in the chABC-treated visual cortex; C: Normal appearance of CSPG-containing PNNs stained with WFA (left); perineuronal and diffuse WFA staining is completely abolished in chABC-treated visual cortex (right). Scale bars: 50 μ m.

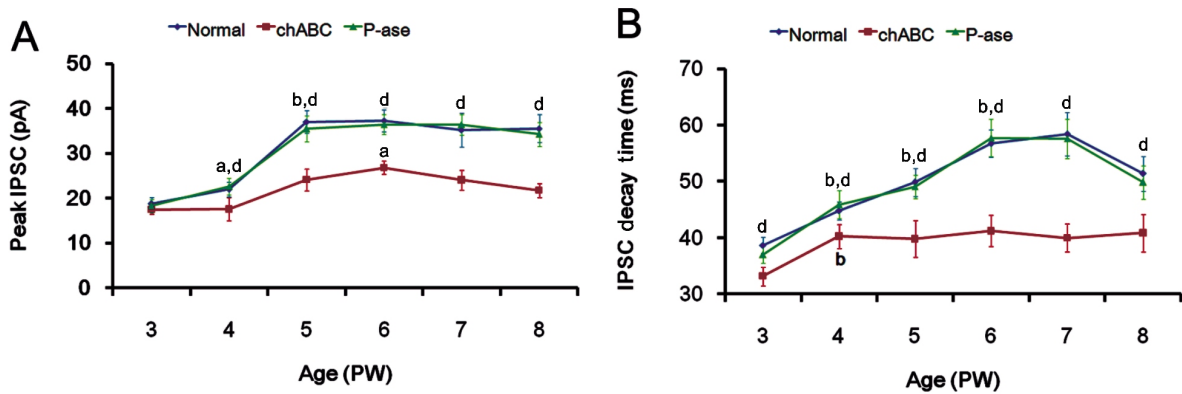


Figure 2 Developmental changes in IPSCs with and without degraded PNNs A: The peak currents of IPSCs in normal rats and rats treated with chABC or P-ase; B: The decay time of IPSCs in normal rats and rats treated with chABC or P-ase. Values are expressed as mean \pm SE, $n=3$ animals per age. ^a $P<0.05$, ^b $P<0.01$ vs the preceding stage, ^d $P<0.01$ between chABC and age-matched control (normal) groups at the same age.

PSCs The marked changes in IPSCs caused by chABC treatment were not observed in total PSCs or in basic membrane properties. Although the peak PSC fluctuated slightly from PW3 to PW8 in the normal and chABC groups, the peak PSCs recorded in the chABC rats were not significantly different from those in the age-matched control rats (Figure 3). PSC decay times showed slight increases from PW3 to PW8 in both groups, but there were no significant differences over time ($P>0.05$, PW3 vs PW8) (Figure 3) or between both groups from PW3 to PW8 (Figure 3). Input resistance (IR) showed a tendency to decrease with age. Although a slightly lower mean IR was shown consistently observed in normal rats, there were no significant differences in IR between normal and chABC rats across ages (Figure 3). Moreover, resting membrane potential (RMP) was not significantly different between the normal and chABC groups at any time point (Figure 3). No differences were observed between the normal and P-ase groups in the peak, decay

time, IR, or RMP properties for total PSCs (Figure 3).

DISCUSSION

Destruction of the PNNs by chABC injection at different stages of rearing dramatically decreased IPSC peak currents and decay times to levels that mimicked those recorded in immature cortex. However, the passive membrane properties were relatively unaffected, as demonstrated by the lack of difference in IR between the normal and chABC-treated groups, and total PSCs were not strongly affected by PNN elimination.

We first investigated developmental changes in GABA_A receptor-mediated inhibition and basic membrane properties of PSCs. We observed developmental increases in peak IPSCs and decay time. The peak IPSCs increased during the critical period and plateaued at PW5 (middle to later stage of the critical period), suggesting that inhibitory synaptic transmission also increased during visual cortex development. Meanwhile, IPSC decay time continued to increase until PW7 (the end of the critical period). These

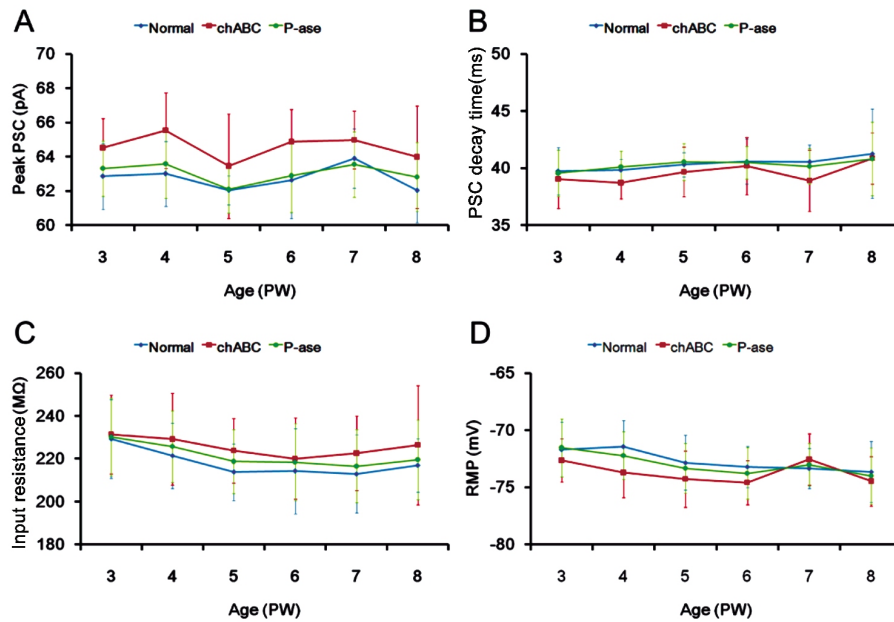


Figure 3 Developmental change in PSCs with and without degraded PNNs A: Peak currents of PSCs; B: PSC decay time; C: PSC input resistance; D: RMP. Blue diamonds, normal; red squares, chABC; green circles, P-ase. Values are expressed as mean \pm SE, $n=3$ animals per age.

results were consistent with the ocular dominance plasticity measured by unit recording^[20] and sweep visually evoked potential^[21], indicating that the postnatal development time course of GABAergic inhibition matched well with that of visual cortex functional maturation. During visual cortex postnatal development^[8,9], inhibitory influences over a certain threshold are necessary for the induction of long-term synaptic plasticity during the early postnatal developmental stage^[10], but further increased inhibition during development suppresses visual cortex neuronal plasticity^[6,11].

However, destruction of the PNNs with chABC injection at different stages of rearing dramatically decreased IPSC peak currents and decay times. The chABC group showed a significant increase in GABAergic currents from PW3 to PW5, whereas currents in normal rats nearly doubled over this period. This rise has been linked with a marked increase in the number of PNNs in all cortical layers at PW5^[8], which could terminate the plasticity of cortical synaptic connections^[22].

Administration of chABC resulted in significantly reduced IPSCs compared with normal rats; IPSCs in chABC-treated rats are maintained at a level that is similar to normal IPSCs at PW3, suggesting the reestablishment of an immature environment for the neurons. GABA becomes inhibitory by the delayed expression of a chloride exporter (KCC2 transporter), leading to a negative shift in the reversal potential for chloride ions^[7]. On the other hand, the observation of the high affinity of anionic iron colloid for perineuronal tissue spaces suggests that PNNs are highly positively charged^[23]. A positively charged net would attract anionic species, including chloride, which would drive the chloride equilibrium potential more negative and possibly

potentiate inhibitory GABA signaling and curtail neuronal plasticity. However, the passive membrane properties were relatively unaffected, as demonstrated by the lack of difference in IR among the three groups, suggesting that total PSCs were not strongly affected by PNN elimination. This finding is consistent with results demonstrating that mice lacking the major adult GABA_A receptor $\alpha 1$ subunit have a normal number of synapses, but retain juvenile IPSC kinetics until adulthood^[24].

The GABA_A receptor $\alpha 1$ subunit participates in the critical period triggered by increasing inhibition; these subunits are enriched at somatic synapses on pyramidal cells made by large-basket parvalbumin interneurons^[25]. As particular subsets of interneurons, parvalbumin neurons play a vital role in dampen pyramidal cell activity by releasing the inhibitory neurotransmitter GABA^[26,27]. Interestingly, most of the cortical neurons possessing PNNs in the visual cortex are parvalbumin neurons^[8]. PNNs may serve as rapid local buffers of excess cation changes in the extracellular space^[28] and subserve fast inhibitory interneuronal actions in visual information processing^[29]. Therefore, our data add a new link between CSPG assembly in PNNs and the functional maturation of GABA receptors.

Acknowledgments: We thank Mr. Chuan-Huang Weng and Dr. Jie Yan for providing technical assistance in patch clamp. We thank Prof. Wei Qin for helpful comments on earlier drafts of the manuscript.

REFERENCES

- 1 Daw NW, Beaver CJ. Developmental changes and ocular dominance plasticity in the visual cortex. *Keio J Med* 2001;50(3):192-197
- 2 Wiesel TN, Hubel DH. Comparison of the effects of unilateral and bilateral eye closure on cortical unit responses in kittens. *J Neurophysiol* 1965;28(6):1029-1040

- 3 Fagiolini M, Hensch TK. Inhibitory threshold for critical-period activation in primary visual cortex. *Nature* 2000; 404(6774): 183-186
- 4 Hensch TK. Critical period plasticity in local cortical circuits. *Nature Reviews* 2005;6(11):877-888
- 5 Huang ZJ, Kirkwood A, Pizzorusso T, Porciatti V, Morales B, Bear MF, Maffei L, Tonegawa S. BDNF regulates the maturation of inhibition and the critical period of plasticity in mouse visual cortex. *Cell* 1999;98 (6): 739-755
- 6 He HY, Hodos W, Quinlan EM. Visual deprivation reactivates rapid ocular dominance plasticity in adult visual cortex. *J Neurosci* 2006;26(11): 2951-2955
- 7 Ganguly K, Schinder AF, Wong ST, Poo M. GABA itself promotes the developmental switch of neuronal GABAergic responses from excitation to inhibition. *Cell* 2001;105(4):521-532
- 8 Pizzorusso T, Medini P, Berardi N, Chierzi S, Fawcett JW, Maffei L. Reactivation of ocular dominance plasticity in the adult visual cortex. *Science* 2002;298(5596):1248-1251
- 9 Bruckner G, Brauer K, Hartig W, Wolff JR, Rickmann MJ, Derouiche A, Delpech B, Girard N, Oertel WH, Reichenbach A. Perineuronal nets provide a polyanionic, glia-associated form of microenvironment around certain neurons in many parts of the rat brain. *Glia* 1993;8(3):183-200
- 10 Bruckner G, Grosche J, Schmidt S, Hartig W, Margolis RU, Delpech B, Seidenbecher CI, Czaniara R, Schachner M. Postnatal development of perineuronal nets in wild-type mice and in a mutant deficient in tenascin-R. *J Comp Neurol* 2000;428(4):616-629
- 11 Hockfield S, Kalb RG, Zaremba S, Fryer H. Expression of neural proteoglycans correlates with the acquisition of mature neuronal properties in the mammalian brain. *Cold Spring Harb Symp Quant Biol* 1990;55: 505-514
- 12 Sur M, Frost DO, Hockfield S. Expression of a surface-associated antigen on Y-cells in the cat lateral geniculate nucleus is regulated by visual experience. *J Neurosci* 1988;8(3):874-882
- 13 Yin ZQ, Crewther SG, Wang C, Crewther DP. Pre- and post-critical period induced reduction of Cat-301 immunoreactivity in the lateral geniculate nucleus and visual cortex of cats Y-blocked as adults or made strabismic as kittens. *Mol Vis* 2006;12:858-866
- 14 Berardi N, Pizzorusso T, Maffei L. Extracellular matrix and visual cortical plasticity: freeing the synapse. *Neuron* 2004;44(6):905-908
- 15 Fritschy JM, Mohler H. GABA_A-receptor heterogeneity in the adult rat brain: differential regional and cellular distribution of seven major subunits. *J Comp Neurol* 1995;359(1):154-194
- 16 Sato MT, Tokunaga A, Kawai Y, Shimomura Y, Tano Y, Senba E. The effects of binocular suture and dark rearing on the induction of c-fos protein in the rat visual cortex during and after the critical period. *Neurosci Res* 2000;36(3):227-233
- 17 Paxinos G. The rat brain in stereotaxic coordinates. New York: Academic Press; 1986:56-59
- 18 Liu YB, Lio PA, Pasternak JF, Trommer BL. Developmental changes in membrane properties and postsynaptic currents of granule cells in rat dentate gyrus. *J Neurophysiol* 1996;76(2):1074-1088
- 19 Wu SH, Fu XW. Glutamate receptors underlying excitatory synaptic transmission in the rat's lateral superior olive studied in vitro. *Hear Res* 1998;122(1-2):47-59
- 20 Fagiolini M, Pizzorusso T, Berardi N, Domenici L, Maffei L. Functional postnatal development of the rat primary visual cortex and the role of visual experience: dark rearing and monocular deprivation. *Vision Res* 1994; 34 (6):709-720
- 21 Guire ES, Lickey ME, Gordon B. Critical period for the monocular deprivation effect in rats: assessment with sweep visually evoked potentials. *J Neurophysiol* 1999;81(1):121-128
- 22 Lander C, Kind P, Maleski M, Hockfield S. A family of activity-dependent neuronal cell-surface chondroitin sulfate proteoglycans in cat visual cortex. *J Neurosci* 1997;17(6):1928-1939
- 23 Murakami T, Ohtsuka A, Matsuoka H, Taguchi T, Abe K, Ninomiya Y. Intensely positively charged perineuronal nets in the adult rat brain as detected by staining with anionic iron colloid. *Arch histol cytol* 2001; 64 (1):45-50
- 24 Bosman LW, Heinen K, Spijker S, Brussaard AB. Mice lacking the major adult GABA_A receptor subtype have normal number of synapses, but retain juvenile IPSC kinetics until adulthood. *J Neurophysiol* 2005;94(1): 338-346
- 25 Katagiri H, Fagiolini M, Hensch TK. Optimization of somatic inhibition at critical period onset in mouse visual cortex. *Neuron* 2007;53(6):805-812
- 26 Kawaguchi Y, Kubota Y. GABAergic cell subtypes and their synaptic connections in rat frontal cortex. *Cereb Cortex* 1997;7(6):476-486
- 27 Somogyi P, Tamas G, Lujan R, Buhl EH. Salient features of synaptic organisation in the cerebral cortex. *Brain Res Brain Res Rev* 1998;26(2-3): 113-135
- 28 Härtig W, Derouiche A, Welt K, Brauer K, Grosche J, Mäder M, Reichenbach A, Brückner G. Cortical neurons immunoreactive for the potassium channel Kv3.1b subunit are predominantly surrounded by perineuronal nets presumed as a buffering system for cations. *Brain Res* 1999;842(1):15-29
- 29 Seeger G, Lüth HJ, Winkelmann E, Brauer K. Distribution patterns of Wisteria floribunda agglutinin binding sites and parvalbumin-immunoreactive neurons in the human visual cortex: a double-labelling study. *J Hirnforsch* 1996;37(3):351-366